New Results from the Reuven Ramaty High Energy Solar Spectroscopic Imager (RHESSI) Mission

R. P. Lin

Physics Department and Space Sciences Laboratory, Univ. of California/Berkeley, Berkeley, CA, USA 94720-7450

Abstract. The primary scientific objective of RHESSI Small Explorer mission is to investigate the physics of particle acceleration and energy release in solar flares, through imaging and spectroscopy of X-ray/gamma-ray continuum and gamma-ray lines emitted by accelerated electrons and ions, respectively. Here we briefly describe the mission and summarize the new solar observations, including the first hard X-ray imaging spectroscopy, the first high resolution spectroscopy of solar gamma-ray lines, and the first imaging of solar gamma-ray lines and continuum.

1. Introduction

The Sun is the most energetic particle accelerator in the solar system, producing ions up to tens of GeV and electrons to hundreds of MeV in solar flares and in fast Coronal Mass Ejections (CMEs). Solar flares are the most powerful explosions, releasing up to 10^{32}-10^{33} ergs in ~10-1000s. The flare-accelerated ~20-100 keV electrons (and sometimes >~1 MeV/nucleon ions) appear to contain a significant fraction, ~10-50%, of this energy, indicating that the particle acceleration and energy release processes are intimately linked. The Reuven Ramaty High Energy Solar Spectroscopic Imager (RHESSI) mission (Lin et al. 2002) provides imaging and spectroscopy of hard X-ray/gamma-ray continua and gamma-ray lines emitted by the accelerated electrons and ions, respectively. At hard X-ray and gamma-ray energies, focusing optics are not feasible. The RHESSI imager (Hurford et al. 2002) is made up of nine Rotating Modulation Collimators (RMCs), each consisting of a pair of widely separated grids mounted on a rotating spacecraft, to achieve angular resolution of ~2 arcsec for hard X-rays and ~35 arsec at gamma-ray energies. Behind each RMC is a segmented germanium detector (GeD), cooled to 75 K to detect photons from 3 keV to 17 MeV with ~keV energy resolution (Smith et al. 2002). As the spacecraft rotates at 15 rpm, the RMCs convert the spatial information from the source into temporal modulation of the photon counting rates of the GeDs. RHESSI was launched on February 5, 2002, into a nearly circular, 38° inclination, 600-km altitude. Over 8000 flares with detectable emission above 12 keV (>~600 above 25 keV) have been observed in the first year, including a gamma-ray line flare. Below we review some of the new results (see the dedicated issues of Solar Physics v. 210, November 2002, and Astrophysical Journal Letters v. 595. no.2, October 1, 2003).

2.   Electron Acceleration and Energy Release in Solar Flares

Figure 1 shows the 20 Feb '02 flare detected by RHESSI. The images, in 2 keV bands from 12 to 26 keV, and then broader bands up to 80 keV (Fig. 2a), show an elongated single source at low energies evolving to two footpoints at high energies. The spatially integrated high-resolution ($\sim$1 keV FWHM) X-ray spectra for the flare (Fig. 2b) shows the thermal hot ($\sim$10 MK) component dominating at low energies, with a power-law component dominating at high energies.

Earlier solar hard X-ray instruments were designed with RHESSI is the first space experiment capable of accurately measuring the flare spectrum from thermal to non-thermal; earlier hard x-ray instruments had thick entrance windows to absorb photons below $\sim$20 or 25 keV to avoid pile-up and saturation (Kane & Anderson 1970). Figure 2b shows the non-thermal power-law spectrum extends down to $\sim$10 keV, implying that the energy contained in the electrons is at least several times greater than estimated previously above $\sim$20 keV (Lin & Hudson 1976). The precise RHESSI observations (Figure 2b) clearly show that the non-thermal spectrum is double-power-law, with a relatively sharp downward break at $\sim$40 keV; a similar break was first seen in the high resolution flare spectrum obtained by a balloon-borne germanium instrument (Lin et al. 1981). The break could be due to a break in the parent electron spectrum due to the acceleration process; or to non-uniform target ionization - the higher energy electrons penetrating to the neutral chromosphere while the lower energy electrons stop in the fully ionized corona where their Coulomb energy loss rate is $\sim$3 times higher (Brown et al. 2002); or some other process.

Surprisingly, the southern footpoint source in Fig 2a peaked about $\sim$8 seconds later than the northern, contrary to the simultaneity generally seen by Sakao et al. (1996). Imaging at $2''$ resolution (Fig. 3), however, shows three sources: source 1 to the north, source 3 to the south, and a weaker, earlier peaking source 2 in-between but much closer to source 3. Source 1 and 2 first brighten simultaneously; then source 3 appears as source 1 peaks and source 2 slowly disappears. Finally, source 3 peaks with a weaker simultaneous brightening of source 1. There also appears to be a fourth source just slightly above the EIT loop (Sui et al. 2002), similar to the weak hard X-ray sources detected in the corona by Yohkoh HXT (Masuda et al. 1994; Alexander & Metcalf 1997) above the soft X-ray loop linking the hard X-ray footpoints. Such sources have been interpreted as evidence for energy release by magnetic reconnection in a region above the soft X-ray loop.

The intense X4.8 flare of 23 July 2002 located at S13E72 is the first gamma-ray line flare observed by RHESSI (Figure 4). The hard X-ray and gamma-ray emission divide naturally into an rise phase ($\sim$0018 to $\sim$0027UT) dominated by a new type of coronal hard X-ray source that appears to be non-thermal, a main impulsive phase ($\sim$0027 to $\sim$0043 UT) with continuum and gamma-ray line emission extending up to $>\sim$7 MeV, and a decay phase ($>\sim$0043UT) dominated by a superhot ($\sim$40 million degrees) thermal hard X-ray source. The spatial distribution of HXR sources (Krucker et al. 2003) is shown superimposed on TRACE 195A images, together with the simultaneous spatially integrated X-ray spectra (Holman et al. 2003), is shown in movie 1 on the accompanying CD and at: http://hesperia.gsfc.nasa.gov/hessi/presentations/video/
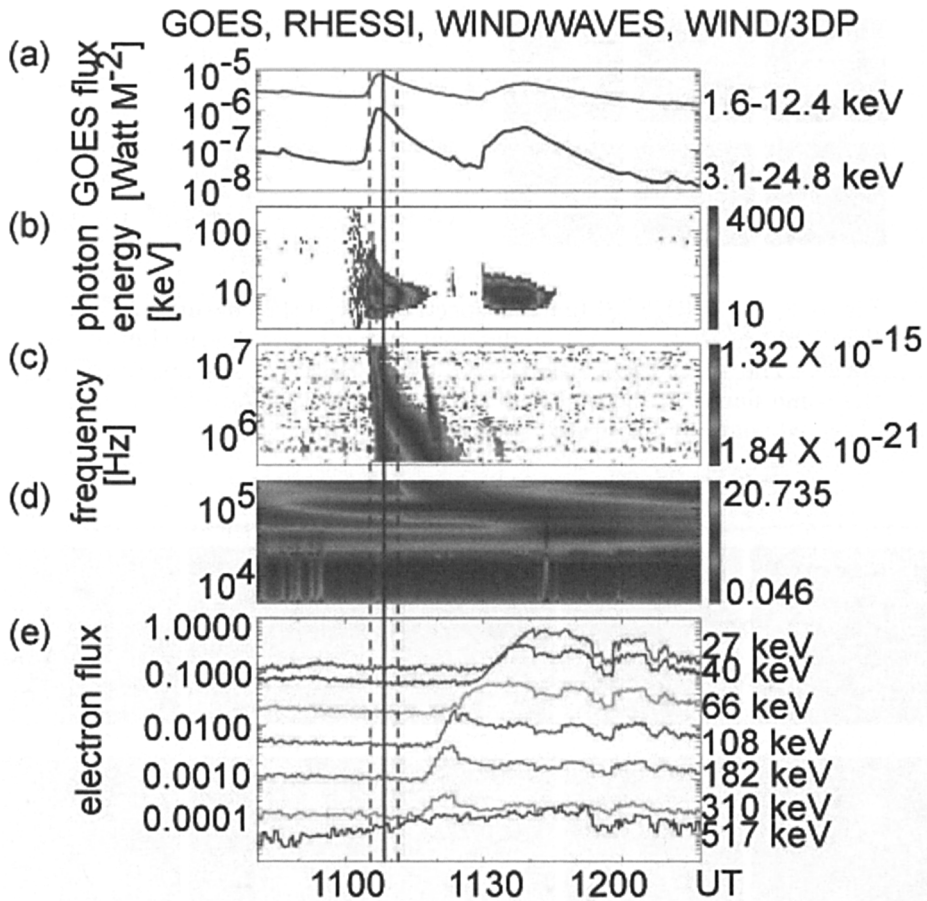
Figure 1. X-ray, radio, and in-situ observations of energetic electrons: From top to bottom the panels show: GOES light curve, RHESSI x-ray spectrogram, WIND/WAVES radio spectrograms, and in-situ electron observations from WIND/3DP (Lin et al. 2002).
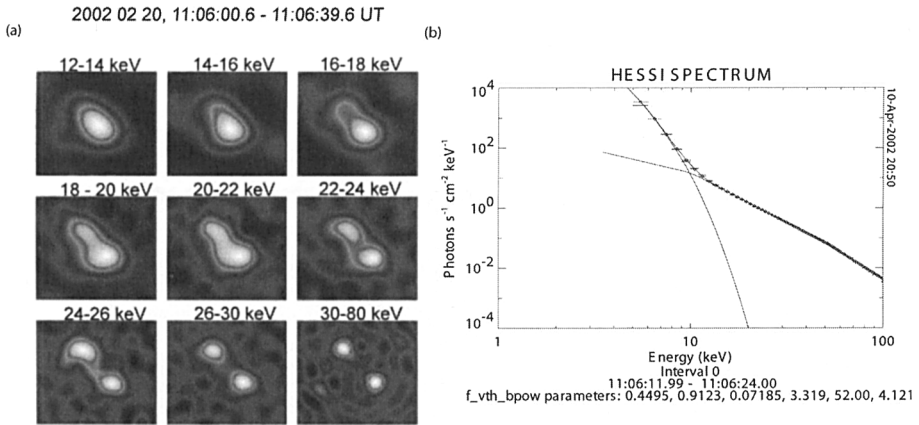
2002 02 20, 11:06:00.6 - 11:06:39.6 UT

(a)   (b)

12-14 keV   14-16 keV   16-18 keV

18 - 20 keV   20-22 keV   22-24 keV

24-26 keV   26-30 keV   30-80 keV

HESSI SPECTRUM

Photons s^{-1} cm^{-2} keV^{-1}

10^4

10^2

10^0

10^{-2}

10^{-4}

1   10   100

Energy (keV)

Interval 0
11:06:11.99 - 11:06:24.00
f_vth_bpow parameters: 0.4495, 0.9123, 0.07185, 3.319, 52.00, 4.121

10-Apr-2002 20:50

Figure 2.   (a) RHESSI Imaging spectroscopy of the February 20, 2002 flare. Images (64″ X 64″) at different energies are shown (Lin et al. 2002). The spatial resolution is 8″. (b) RHESSI X-ray spectrum of the same flare. A thermal and a broken power law are fitted to the observed spatially integrated spectrum.

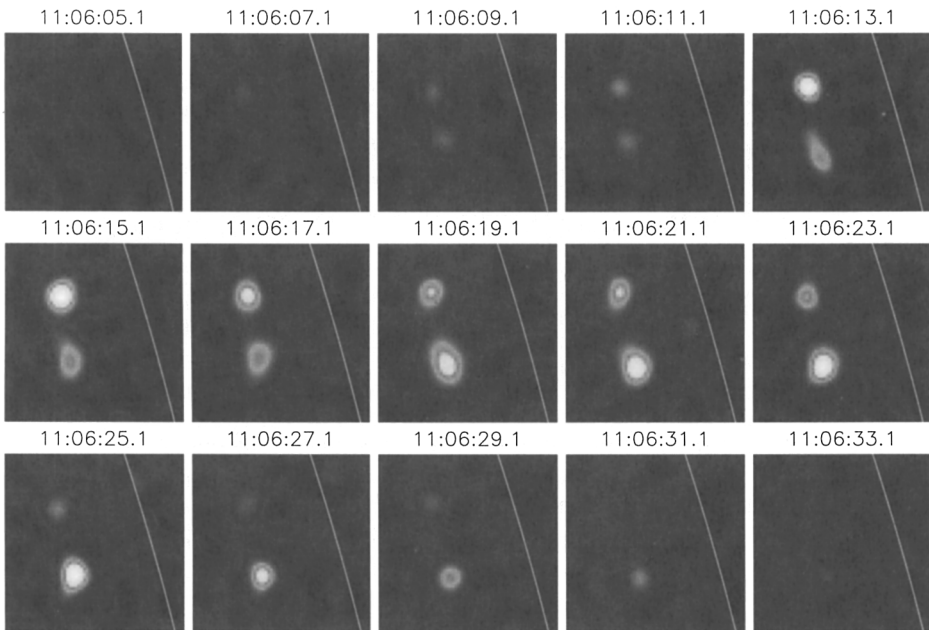| 11:06:05.1 | 11:06:07.1 | 11:06:09.1 | 11:06:11.1 | 11:06:13.1 |
| 11:06:15.1 | 11:06:17.1 | 11:06:19.1 | 11:06:21.1 | 11:06:23.1 |
| 11:06:25.1 | 11:06:27.1 | 11:06:29.1 | 11:06:31.1 | 11:06:33.1 |

Figure 3.   Images for 20-40 keV band at 2″ resolution for the 20 February 2002 flare, shown at 2 s cadence.
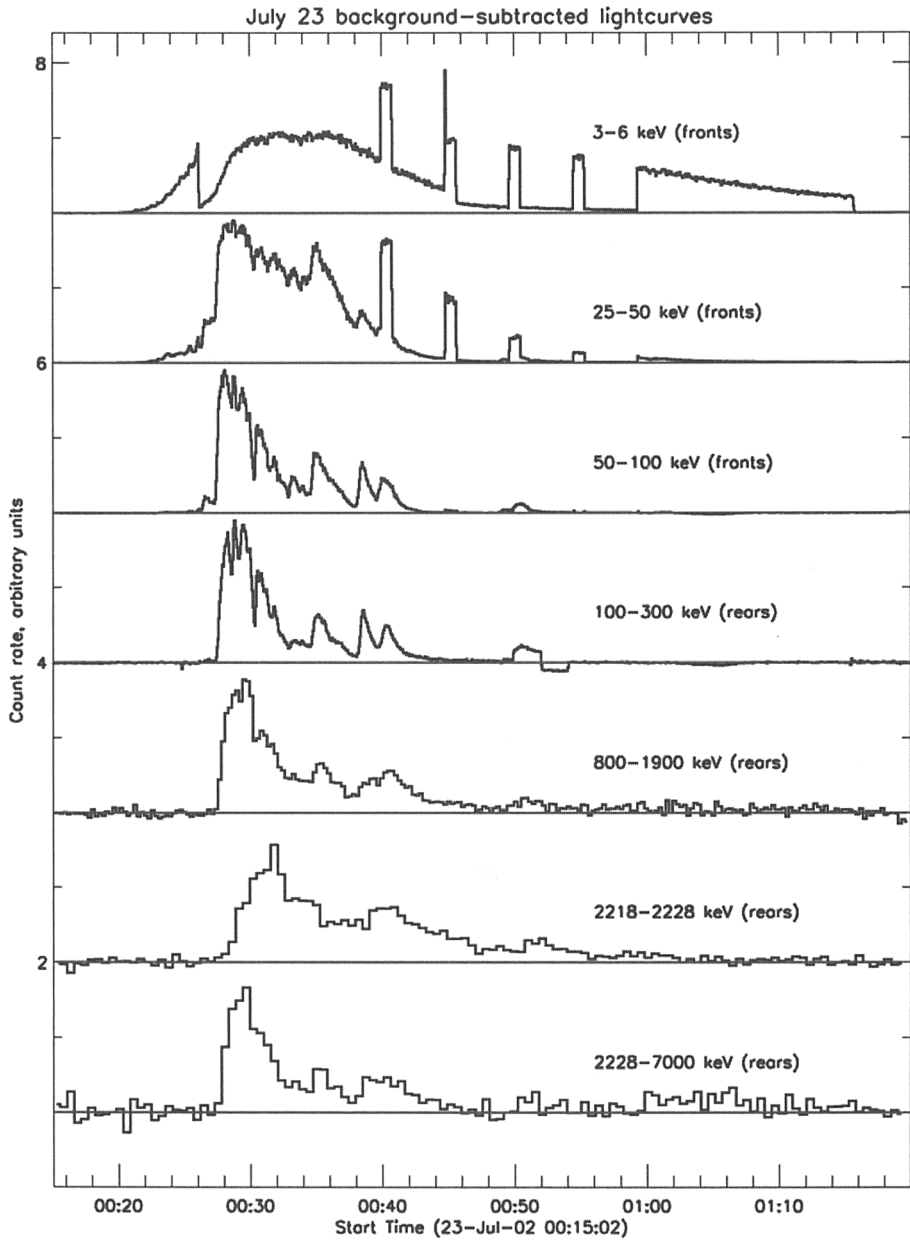
Figure 4.   Background-subtracted light curves for the July 23, 2002 gamma-ray flare at 7 different energies.

During the rise the hard X-ray emission above 10 keV is concentrated in an unusual coronal source (see movie) with no counterpart observed in TRACE 195 A, SOHO MDI visible or Hα images (Lin et al. 2003). The hard x-ray spectrum above $\sim$10 keV fits to a double-power-law spectral shape (Holman et al. 2003). Assuming thick target emission from energetic electrons colliding with a cold ambient medium (E_e>>kT), the energy deposited by the electrons above $\sim$10 keV, integrating over time from the rise to $\sim$0026UT, is $>\sim 4\times 10^{32}$ ergs. But by fitting the observed spectrum to a thermal component plus a power-law non-thermal component, and choosing the highest possible low energy cutoff ($\sim$20 keV) to the non-thermal electron spectrum that is consistent with the X-ray data, Holman et al. finds a lower limit to the total energy input in accelerated electrons of $\sim 2\times 10^{31}$ ergs. Thus, very substantial energy release and acceleration of electrons occurs high in the corona prior to the impulsive phase.

At the beginning of the impulsive phase, $\sim$0027UT, there is an abrupt change in the character of the hard X-ray emission, to strong footpoint emission (Krucker et al. 2003) together with a (super)hot thermal source in the corona (see movie). Three footpoints are observed - a north, a south, and a middle footpoint - each with a chromospheric counterpart observed in Hα and TRACE. Their spectra, although still double-power-law, are much harder than the rise phase coronal source. During the first (and most intense) burst, the north footpoint rapidly moves northeast, roughly parallel to the magnetic neutral line, while the south footpoint stays relatively stationary, so the separation between them increases with time. These X-ray fluxes and spectra of the north and south footpoints show the same temporal variations, suggesting that they are at opposite ends of the same magnetic loop. The motions generally are most rapid when the X-ray flux is largest, as might be expected if magnetic reconnection is forming the loops connecting the footpoints and the rate of electron acceleration is related to the reconnection rate.

3.   Ion Acceleration and Gamma-ray Line Emission

RHESSI has provided the first direct information on the location and spatial characteristics of the accelerated ions in a flare, by imaging the gamma-ray line emission produced by collisions of the energetic (tens of MeV) ions with the ambient solar atmosphere (Hurford et al. 2003). The two rotating modulation collimators (35 & 180 arcsec resolution) with the thickest (2 & 3 cm, respectively) tungsten grids were used to obtain images of the narrow deuterium line at 2.223 MeV formed by thermalization and capture of neutrons produced in the collisions, the 3.25-6.5 MeV band that includes the prompt de-excitation lines of C and O, and the 0.3-0.5 and 0.7-1.4 MeV bands that are dominated by electron-bremsstrahlung, all for the same time interval.

The centroid of the 2.223 MeV image (Figure 5) was found to be displaced by $\sim$20($\pm$6) arcsec ($\sim$15,000 km) from that of the 300-500 keV band (and from the 50-100 keV X-ray continuum emission), implying a difference in acceleration and/or propagation between the accelerated electron and ion populations near the Sun. The de-excitation lines, which come from ambient nuclei stimulated by accelerated protons and alpha particles, were measured for the first time with high spectral resolution (Figure 6) (Smith et al. 2003). They were discovered
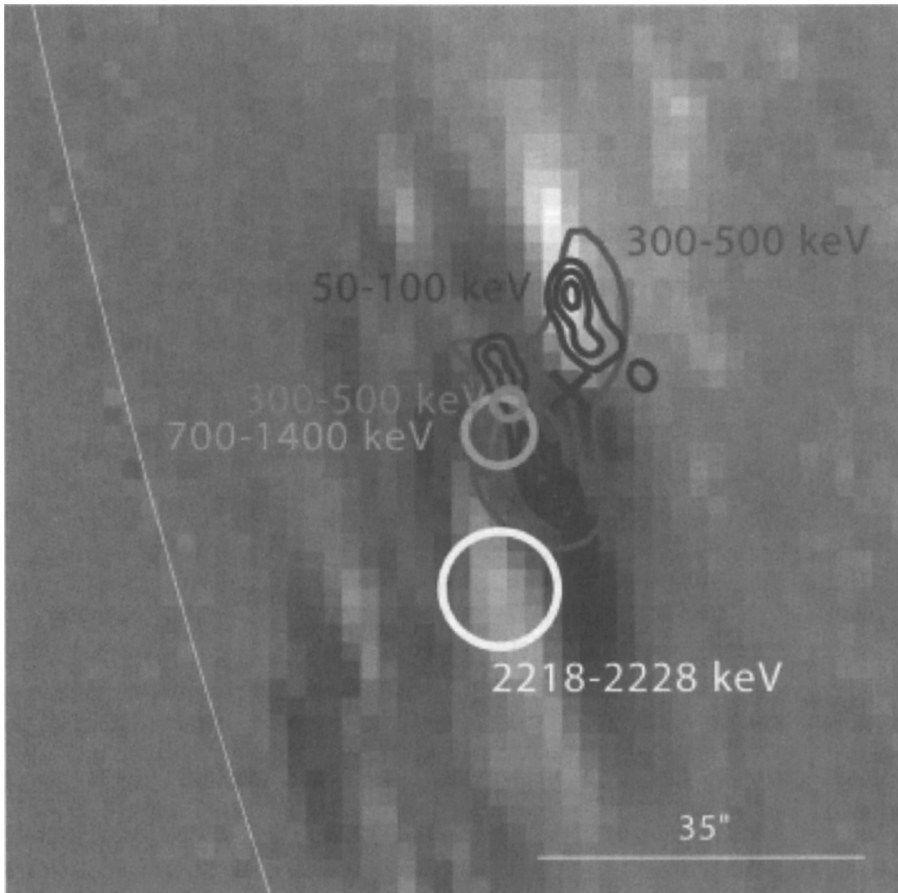
Figure 5. Location of the gamma-ray source for the 23 July 2003 flare (Hurford et al. 2003). The circles represent the 1-sigma errors for the energies given. All these images are made with identical imaging parameters. The FWHM angular resolution is shown in the lower right. Black contours show the high resolution 50-100 keV map at 3″ resolution and the gray contours represents the 300-500 keV map with 8″ resolution. The black X shows the centroid of the 50-100 keV emission made with the same lower resolution as the gamma-ray maps. The background is a TRACE 195A image of the post-flare loops.
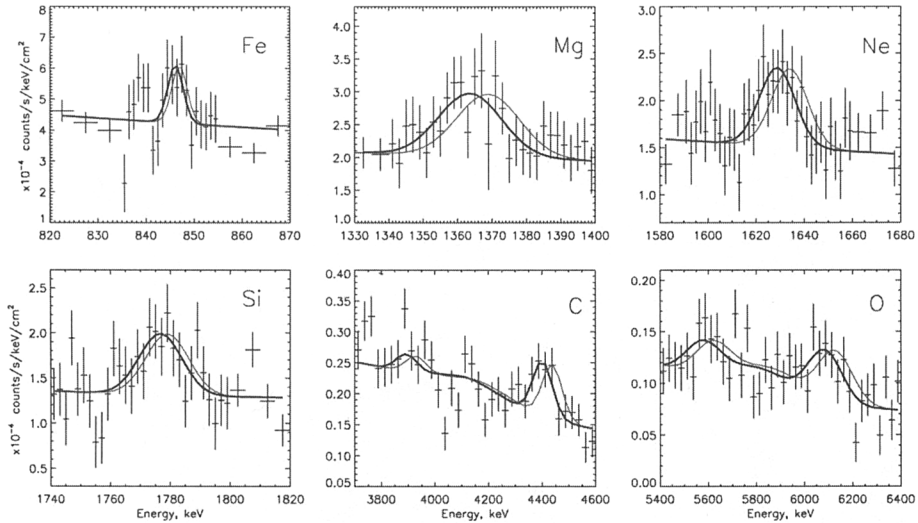
Figure 6.   RHESSI background-subtracted count spectra from 00:27:20UT to 00:43:20UT on 23 July, 2002 (Smith et al. 2003). For the narrow gamma-ray lines of C, O, Mg, Ne, Si, and Fe. The heavy line in each panel is a Gaussian fit plus the underlying bremsstrahlung continuum and broad lines, convolved with the instrument response. The lighter line is the same fit forced to zero redshift for comparison. The error bars are from Poisson statistics.

to be significantly redshifted, by fractions of a percent, even though the flare was nearly on the solar limb. These redshifts imply that the magnetic loop containing the ions must have been strongly tilted from radial, toward the solar surface.

4.   Microflares and the Quiet Sun

The Sun releases energy in transient outbursts, ranging from major flares down to microflares and even nanoflares, with the frequency of the releases increasing as the energy released decreases (see discussion in Aschwanden et al. 2000). Hard X-ray microflares, tiny bursts with 10^{27} to 10^{28} ergs in >20-keV electrons, were discovered to occur on average once every ~6 minutes near solar maximum (Lin et al. 1984), leading to speculation that the energy released in accelerated electrons, summed over HXR bursts of all sizes, might contribute significantly to the heating of the active corona. With BATSE SPEC observations with 8 keV thresholds, Lin et al. (2001) found that only one third of all non-thermal (hard spectra unlikely to be thermal) events detected above 8 keV are observed above 25 keV. The generally steep HXR spectra (power-law fits with exponent of 3-7) reveal that most of the flare energy is contained in the non-thermal electrons at lowest energy. The RHESSI instrument accommodates medium and large flares by automatically inserting shutters in front of detectors to absorb low energy
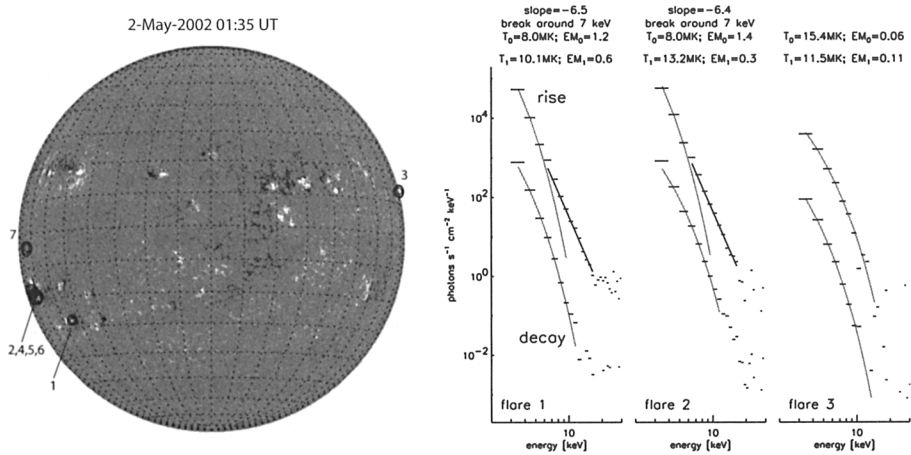
Figure 7. (left) Locations of the 7 largest microflares (GOES class A6 and smaller) observed (Krucker and Lin 2002). (right) Spectra during the impulsive phase (shown shifted up by two decades) and the decay phase of the microflares labeled 1 to 3 in the figure to the right. The impulsive phase is fitted with both a thermal (light gray) and a non-thermal (dark gray) component, the decay phase with a thermal component only. For the behind-the-limb microflare (flare 3), a thermal alone fits the data well enough. The shown colored curves give the range fitted; values above ~15 keV are dominated by noise.

photons and avoid saturation. RHESSI with the shutters out has an effective area 14 to 500 times larger than the most sensitive previous instrument from 3 to 15 keV, the Hard X-ray Imaging Spectrometer (HXIS) on SMM.

Figure 7 shows the locations of the 7 largest microflares (GOES class A6 and smaller) observed from 1:40 to 2:40 UT on May 2, 2002. These have soft (power law exponents between 4 and 7) non-thermal spectra down to low (<~7 keV) energies (Benz & Grigis 2002; Krucker et al. 2002). If a 25 keV cutoff energy is assumed, the total energy in non-thermal electrons in microflares is underestimated by at least a factor of ~10, in some events up to a factor of ~2000. Furthermore, the smaller the event, the steeper the spectrum appears to be. Thus there may be a systematic underestimate of the energy in small events relative to large events, and the frequency distribution of microflares may well be steeper than previously reported (Crosby et al. 1993), i.e. microflare heating might contribute more to coronal heating than previously thought.

5. Hard X-ray Emission from Type III Radio Bursts

Type III solar radio bursts are emitted by energetic electrons escaping from the Sun. The electrons excite Langmuir waves, which in turn generate radio emission at the plasma frequency and/or its harmonic. As the electrons travel outwards into lower density regions, the radio emission exhibits a characteristic fast drift to lower frequencies. Type III bursts are often observed with flares, but

most occur in the absence of flares and vice-versa. The flare-associated type III bursts generally occur in close temporal coincidence with the flare HXR burst. Both the energetic electrons and the Langmuir waves have been detected in situ at 1 AU, but the number of electron escaping to 1 AU is typically $\sim$0.1% of the number required to produce >20keV HXR emission detectable by previous solar hard-ray instruments. With RHESSI's uniquely high sensitivity down to 3 keV, however, very weak HXR bursts are often observed coincident with type III bursts (Figure 8). These HXR bursts are not associated with a reported flare, and often no flaring soft X-ray (SXR) emission is detected by GOES. This weak HXR emission may be the bremsstrahlung emission produced by the escaping type III electrons. The lack of flare SXR and optical emission suggests that type III bursts may be a phenomenon independent of, but often triggered by flares.

These escaping electrons can be used to unambiguously trace magnetic field lines, through imaging by RHESSI of the X-rays they produce, with radio tracking of the Type III emission they produce from the Sun to 1 AU, and then detection of the $\sim$keV to few tens of keV electrons themselves (see Fig. 1).

6.   Flare/CME Associations

Little is understood about the early initiation of a CME and its connection to the very large energy release of the often-associated flares. RHESSI has provided observations of several such associated flares in which 10^{32} ergs or more appear in the nonthermal electrons alone on time scales of minutes during the period of CME initiation and acceleration. In the flare/CME event on 21 April 2002 (see movie 2 in the accompanying CD) the first hard X-ray emission was detected with RHESSI some 5 minutes before any brightening was observed in the TRACE 19.5-nm images (Gallagher et al. 2002), presumably because the early hot plasma was at a higher temperature than the $\sim$1.5 MK sensitive range of the TRACE passband. The hard X-ray emission continued to rise for the following hour, at the same time that a wave-like propagation appeared to move through the TRACE field at a mean velocity of $\sim$120 km/s. This has been interpreted by Gallagher et al. (2003) as the first evidence for the CME. Gallagher et al. (2003) combined SOHO CME observations to show that the leading edge of the CME accelerated to a maximum velocity of over 2500 km/s in less than 2 hours. The maximum rate of acceleration was as high as 1500 m/s^2 and this occurred when hard X-ray emission was seen with RHESSI. The flare released some 10^{32} ergs during its rise phase over the same time period that the CME was being accelerated. An intense SEP event was seen at the Earth.
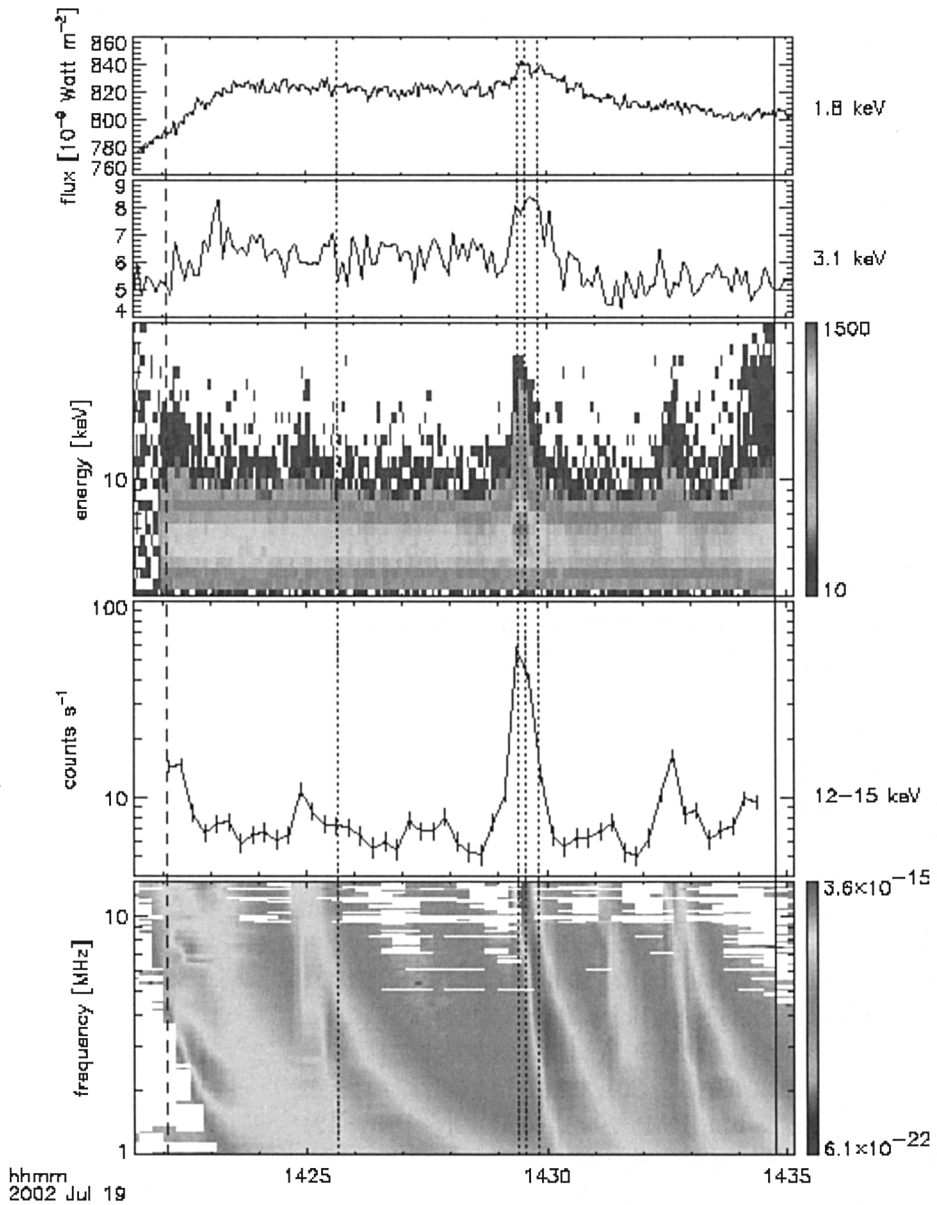
Figure 8.   X-ray and radio observations of several type III radio and hrad X-ray bursts. From top to bottom, GOES lightcurves, RHESSI X-ray spectrogram, RHESSI 12-15 keV lightcurve, and WIND/WAVES radio spectrogram are shown.

tists on the HESSI team are David Smith, Jim McTiernan, Isabel Hawkins, Said Slassi-Sennou, Andre Csillaghy, George Fisher, Chris Johns-Krull (now at Rice University) at Berkeley; Richard Schwartz, Larry Orwig, Dominic Zarro at Goddard Space Flight Center; Ed Schmahl at University of Maryland; and Markus Aschwanden at Lockheed-Martin. The engineering team at Berkeley is led by Peter Harvey and include Dave Curtis, and Dave Pankow; at GSFC, Dave Clark and Rob Boyle; at PSI, Reinhold Henneck, Akilo Michedlishvili, and Knut Thomsen. The HESSI spacecraft is being developed and fabricated by Spectrum Astro Inc. The project manager for HESSI in the GSFC Explorer Office is Frank Snow. This research is supported by NASA contract NAS5-98033 to the University of California, Berkeley.

References

Alexander, D. & Metcalf, T. R. 1997, ApJ, 489, 422

Aschwanden, M. J. et al. 2000, ApJ, 535, 1047

Aschwanden, M. J. et al. 2002, Solar Phys., 210, 193

Benz, A. O. & Grigis, P. C. 2002, Solar Phys., 210, 431

Brown, J. C. et al. 2002, Solar Phys, 210, 373

Cane, H. V. et al. 2002, J. Geophys. Res., 107, SSH 14-1, CiteID 1315

Coburn, W. & Boggs, S. 2003, Nature, 423, 415

Crosby, N. B. et al. 1993, Solar Phys., 143, 275

Drake, J. F. et al. 2003, Science, 299, 873

Emslie, A.G. 2003, ApJ, 595, L119

Gallagher, P.T. et al. 2002, Solar Phys., 210, Nos. 1-2, 341

Gallagher, P. T. et al. 2003 ApJ, 588, 53

Golpaswamy, N. et al. 2002, ApJ, 572, 103

Gordovsky, M. & Zharkova, V.V. 2003, National Astronomy Meeting (NAM), Dublin, Ireland

Holman, G. D. et al. 2003, ApJ, 595, L97

Hurford, G. H. & Curtis, D. 2002, Solar Phys., 210, 101

Hurford, G. et al. 2002, Solar Phys., 210, 61

Hurford , G.J. et al. 2003, ApJ Lett., 595, L77

Hurley, K. 2002, BAAS, 201, 69.01

Johns, C. M. & Lin, R. P. 1992, Solar Phys., 137, 121

Kahler, S. 1999, ApJ, 428, 837

Kane, S. R. & Anderson, K. A. 1970, ApJ, 162, 1003

Klein, K.-L. et al., 2001

Kosugi et al. 1991, Solar Physics, 136, 17

Krucker, S. et al. 2002, Solar Phys., 210, Nos. 1-2, 445

Krucker, S. et al. 2003, ApJ, 595, L103

Larson, D. et al. 2000, AGU, Spring Mtg, abstract #SH61A-09

Lin, R. P. 1985, Solar Phys., 100, 537

Lin, R. P. 1987, Reviews of Geophysics, 25, 676

Lin, R. P. 1994, EOS Trans, AGU, 75, #40, 457

Lin, R. P. & Hudson, H.S. 1976, Solar Phys., 50, 153

Lin, R. P. et al. 1984, ApJ Lett., 251, L109

Lin, R. P. et al. 1996, Geophys. Res. Lett., 23, 1211

Lin, R. P. et al. 2001, ApJ, 557, L125

Lin, R. P. et al. 2003, ApJ, 595, L69

Makishima et al. 1977, New Instrumentation for Space Astronomy, K. A. van
    der Hucht & G. Vaiana eds., New York: Pergamon Press

Mandzhavidze, N. et al. 1999, ApJ, 518, 918

McConnell, M. L. et al. 2002, Solar Phys., 210, Nos. 1-2, 125

Murphy, R. J. et al. 1991, ApJ, 371, 793

Oieroset, M. et al. 2002, Physical Sci. Rev., 89, id. 195001

Piana, M. et al. 2003, ApJ, 595, L127

Prince, T.A. et al. 1988, Solar Phys., 118, 269

Rauscher, E. et al. 2002, AGU Fall Mtg., abstract #SH52A-0482

Reames, D. V., 1996, ApJ Lett. 466, 473

Reames, D. V. et al. 1985, ApJ Lett., 292, 716

Schmahl, E. J. & Hurford, G. J. 2002, Solar Phys. 210, Nos 1-2, 287

Schwartz, R. A. et al. 2002, Solar Phys., 210, 165

Share, G. H. et al. 2002, Solar Phys., 210, Nos. 1-2

Share, G. H. et al. 2003, ApJ, 595, L89

Shimizu, T. 1995, PASJ, 47, 251

Smith, D. M. 2003, ApJ, 589, L55

Smith, D. M. et al. 2003, ApJ, 595, L81